Identification of Photon-tagged Jets in the ALICE Experiment

G. Conesa [a,b,*] H. Delagrange [b] J. Díaz [a] Y.V. Kharlov [c]

Y. Schutz [b,d]

[a] *IFIC (Centro Mixto Universidad de Valencia-CSIC), Valencia, Spain*

[b] *SUBATECH, Ecole des Mines, IN2P3/CNRS, Université de Nantes, Nantes, France*

[c] *Institute for High-Energy Physics, Protvino, Russia*

[d] *CERN, Genève, Switzerland*

Abstract

The ALICE experiment at LHC will detect and identify prompt photons and light neutral-mesons with the PHOS detector and the additional EMCal electromagnetic calorimeter. Charged particles will be detected and identified by the central tracking system. In this article, the possibility of studying the interaction of jets with the nuclear medium, using prompt photons as a tool to tag jets, is investigated by simulations. New methods to identify prompt photon-jet events and to distinguish them from the jet-jet background are presented.

Key words: High-energy gamma rays, electromagnetic calorimeters, quark-gluon plasma.

PACS: 25.75.Nq, 24.10.Lx, 25.75.-q, 29.40.Vj

1 Introduction

In Ref. [1], we stressed the importance of the measurement of jets in the ALICE experiment at LHC to study the properties of the nuclear medium predicted to be created in ultra-relativistic heavy-ion collisions, the Quark-Gluon Plasma [2, 3]. Jets will be abundantly produced at the LHC (2×10^6 jets with $p_T > 100$ GeV/c per year in the ALICE acceptance) enabling inclusive and exclusive jet measurements. In particular, jet topology (jet shape, jet *heating*, fragmentation function,...) can be measured to study the redistribution of the jet energy among the fragmentation particles after the jet has traversed the nuclear medium created in the collision [4]. These studies require the identification of jets and the measurement, as accurately as possible, of the jet energy, ideally before and after interaction with the medium. A very attractive method to perform these studies is to tag jets with prompt photons emitted opposite to the jet direction. The dominant processes for such events are $g + q \rightarrow \gamma + q$ (Compton) and $q + \bar{q} \rightarrow \gamma + g$ (annihilation), although recent studies show that Next to Leading Order processes (NLO) contribute significantly to the photon spectrum below 50 GeV/c [5]. As photons emerge almost unaltered from the dense medium, they provide a measurement of the original energy of the parton emitted in the opposite direction. On one hand, this coincidence technique can be used to localize the jet and on the other hand it allows to build the parton fragmentation function without the need of reconstructing the jet energy from the detected hadrons. Medium effects can then be identified through modifications of the fragmentation function, i.e., by the redistribution of the jet energy among its components.

* Corresponding author
Email address: Gustavo.Conesa.Balbastre@cern.ch (G. Conesa).

The identification of prompt photons in ALICE with the high resolution photon spectrometer PHOS in association with the central tracking system has been presented earlier [1,6]. The identification of prompt-photon jet events in ALICE is found optimal for photons with energy larger than 20 GeV. Below this energy, decay and prompt photons cannot be efficiently separated on an event by event basis.

In this paper, we discuss the possibilities offered by the addition of the EMCal electromagnetic calorimeter to the ALICE setup. We present an algorithm for identifying photon-jet events and for reconstructing hadron jet features. The algorithm was developed and tested with the simulations described in Ref. [1]. The study was done with generated particles reconstructed with a fast reconstruction algorithm, due to lack of computer time for a full reconstruction. The generator used to produce pp collisions at $\sqrt{s}$ = 5.5 TeV is PYTHIA 6.203 [7,8]. The simulations generated with PYTHIA contain γ-jet and jet-jet events, with prompt and decay photons, respectively, in the energy range 20$<$E$<$100 GeV. The generator used to reproduce the underlying event of a heavy-ion collision is HIJING 1.36 [9]. To show the improvements provided by the electromagnetic calorimeter EMCal in the jet reconstruction procedure, two possible experimental situations are considered: i) only charged particles can be detected (EMCal is not present) and ii) neutral particles can also be detected (EMCal is present).

2 Acceptance and response of the detectors

To assess the performance of our photon-jet identification algorithm, a fast detector simulation is used because a complete event simulation with particle

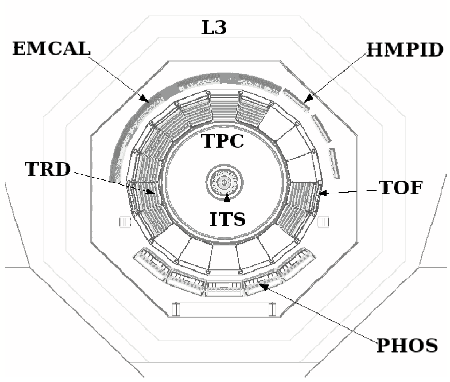

Fig. 1. Sketch of the ALICE experiment, transverse view.

transport and reconstruction would have required an unaffordable computing time. In this fast simulation framework, we rely only on the properties of the final state particles generated by PYTHIA and on the knowledge of the response function and acceptance of the various detectors involved.

The ALICE experiment is sketched in Fig. 1. The acceptances of all the detectors relevant for this study are listed in Table 1. A full description of the ALICE detector can be found in Ref. [10].

The response function of the detectors involved in our analysis, PHOS and the central tracking system (TPC), are described in Sec. 3 of Ref. [1]. The EMCal response was assumed to be identical to the PHOS response, although in fact it will be slightly worse. However, since the EMCAL granularity is coarser, the p_T range over which a Shower Shape Analysis (SSA) can discriminate prompt photons from decay photons [1] is reduced from about 100 GeV/c in PHOS down to 40 GeV/c in EMCal.

[1] Due to Lorentz contraction and the calorimeters granularity decay photons merge in one detected cluster for $E_{\pi^0} \gtrsim 30$ GeV in PHOS and $E_{\pi^0} \gtrsim 10$ GeV in EMCal.

Table 1

TPC (Time Projection Chamber), PHOS and EMCal acceptances. The physical TPC η acceptance is larger ($|\eta| < 0.9$), but we take this lower value to ensure a good track matching. The acceptance of EMCal used in this study might not be the final one as the layout is still under discussion.

Detector	$\lvert\eta\rvert$	ϕ_{min}	ϕ_{max}
PHOS	0.12	220°	320°
EMCAL	0.7	60°	180°
TPC	0.7	0°	360°

3 Jet selection procedure

Photon-jet events were identified by applying the following γ-tagging algorithm:

(1) Find the most energetic prompt photon identified in PHOS (Ref. [1]).

(2) Find the jet leading particle [2], either a charged hadron detected by the central tracking system or a neutral pion detected by the EMCal, with the highest p_T value and emitted back-to-back to the photon ($\Delta\phi \sim 180°$). Neutral pions are identified from their two photon decay from all photons in the event with a relative angle between the limits defined by the decay kinematics and with an invariant mass in the range $120 < M_{\gamma\gamma} < 150$ MeV$/c^2$. In addition, it is required that the p_T value of the leading particle be at least 10% of the photon energy.

(3) Reconstruct the jet as the ensemble of all particles above a given p_T

[2] Jets always have a particle carrying a significant fraction of the jet energy (in average 40%).

threshold contained inside a cone of a given radius around the leading particle direction.

(4) Finally, the event is identified as a photon-jet if the ratio of the reconstructed jet energy and the prompt photon energy falls within a given selection window.

There are standard algorithms that can be used to reconstruct jets (k_T, cone, etc), but they fail to reconstruct jets with energy smaller than 40-50 GeV in a heavy-ion environment [6, 11]. Studies about tagging reconstructed jets with prompt photons with standard algorithms are in progress.

3.1 Leading particle selection

In ALICE, since the central tracking system and EMCal do not cover the same acceptance, jets can be fully reconstructed (charged plus neutral hadrons) only over a limited solid angle ($|\eta| < 0.7$ and $\Delta\phi = 120°$ in this study [3]). Therefore, outside the common acceptance region, the jet energy is only partially reconstructed which may lead to the rejection of a true γ-jet event.

The prompt photon and the parton at the origin of the observable γ-jet event are emitted in opposite directions in the center of mass of the hard process. In the laboratory system, the correlation in pseudo-rapidity is washed out, as illustrated in Fig. 2, while the azimuthal angle correlation is conserved since there is no boost in the transverse direction. The relative azimuthal angle, $\Delta\phi$, of γ-jet events is peaked at 180° and its width depends on both the

[3] The EMCal design is still under discussion and now, an azimuthal aperture of 110° is considered.

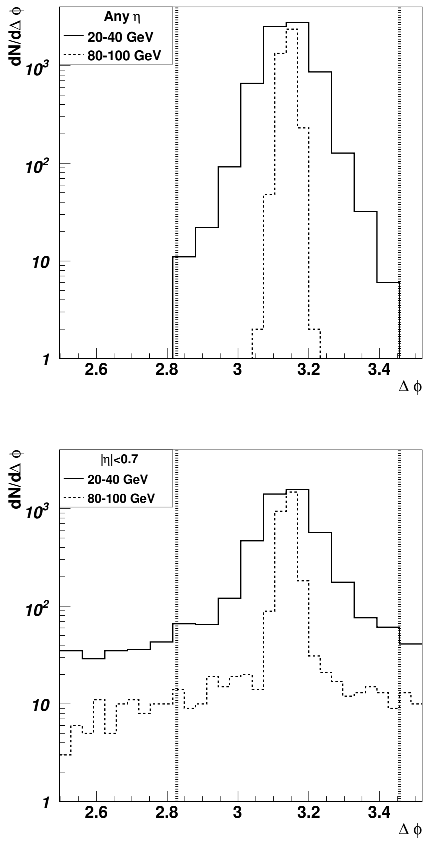

Fig. 2. Azimuthal angle correlations between prompt photons and their corresponding jet leading particles as a function of $\Delta\phi = \phi_l - \phi_\gamma$ for simulated γ-jet events in the energy ranges 20-40 GeV and 80-100 GeV for pp collisions. Jet particles (lower frame) are filtered through the acceptance $|\eta| < 0.7$. Dotted vertical lines represent the cut between 0.9π and 1.1π that we use to select leading particles.

detector acceptance and resolution, and the energy of the event. We have tuned our algorithm to select photon leading-particle pairs satisfying the angular condition $0.9\,\pi < \Delta\phi < 1.1\,\pi$.

When the leading particle of a given event escapes from the detector acceptance, the algorithm finds a wrong leading particle. This misidentification produces the peak in the jet leading particle distribution at low values of the $p_{T,l}/E_\gamma$ ratio (Fig. 3), where $p_{T,l}$ and E_γ are the momentum of the identified

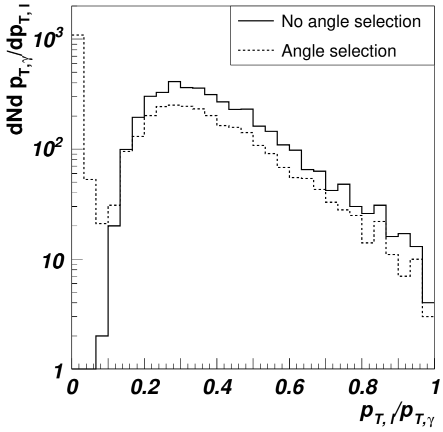

Fig. 3. Leading particle distribution of γ-jet events as a function of the $p_{T,l}/E_\gamma$ ratio for pp collisions and jet energies in the range 80 -100 GeV. The dotted line corresponds to the case where the leading particle is searched inside the acceptance of the detectors and opposite in ϕ angle to the prompt photon. The solid line corresponds to the case whithout acceptance restrictions.

leading particle and the energy of the photon, respectively. These fake leading particles are rejected by imposing the condition $p_{T,l}/E_\gamma > 0.1$. The probability of finding the jet associated to a prompt photon is about 50%, determined only by the jet detection acceptance.

3.2 Identification of π^0 leading particles

The π^0 candidates to leading particles are identified by detecting their two decay photons in EMCal and selecting those with an invariant mass $M_{\gamma\gamma}$ around the π^0 rest mass. Because of the combinatorial background, which is particularly large in the case of Pb-Pb collisions (Fig. 4), additional selection conditions are necessary.

The opening angle θ_{12} between the two π^0 decay photons is given in the lab system by:

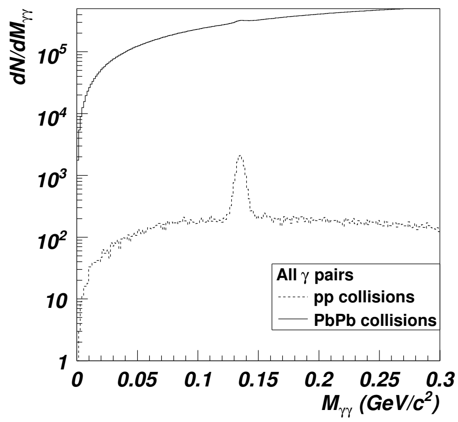

Fig. 4. Invariant mass distributions of all photon pairs in the event for pp (dashed line) and Pb-Pb (solid line) collisions at $\sqrt{s} = 5.5A$ TeV. No selection is applied.

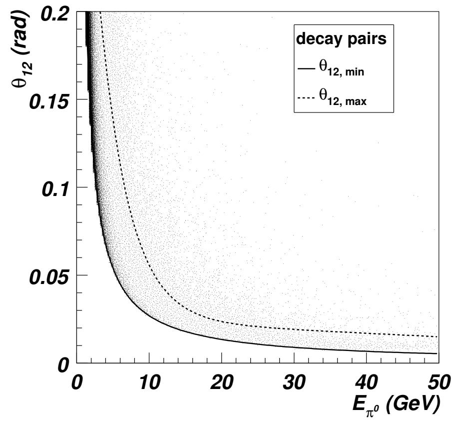

Fig. 5. Opening angle of π^0 decay photon pairs (without any restriction in detector acceptance). The lines limit the opening angle range selected; the lower line is obtained from the decay kinematics, the upper one has been empirically chosen to select most of π^0 decay pairs.

$$\cos\theta_{12} = \frac{\gamma_\pi^2\beta_\pi^2 - \gamma_\pi^2\alpha^2 - 1}{\gamma_\pi^2(1-\alpha^2)}, \tag{1}$$

where α is the decay asymmetry, γ, the Lorentz factor and β the π^0 velocity in units of c. The opening angle is minimum for symmetric decays ($\alpha = 0$). From the simulated π^0 opening angle distributions in Pb-Pb collisions (Fig. 5),

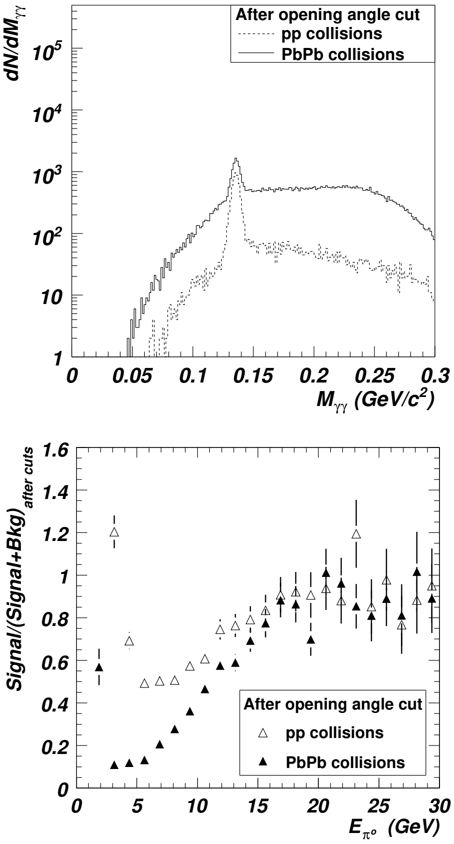

Fig. 6. Upper frame: Invariant mass distributions of photon pairs in the event which satisfy the ϕ and leading particle energy cuts and the opening angle restriction, for pp (dashed line) and Pb-Pb (solid line) collisions at $\sqrt{s} = 5.5A$ TeV. Lower frame: Ratio of the simulated π^0 number to the selected photon pair number in the event, for pp ($\triangle$) and Pb-Pb ($\blacktriangle$) collisions at $\sqrt{s} = 5.5A$ TeV. Only γ-jet events with jet energy in the range from 20 to 100 GeV are considered.

the maximum opening angle was empirically selected by fitting the equation

$$\theta_{max} = 0.4 \cdot e^{-0.25 \cdot E} + 0.025 - 2 \cdot 10^{-4} \cdot E_{\pi^o}. \quad (2)$$

to the data.

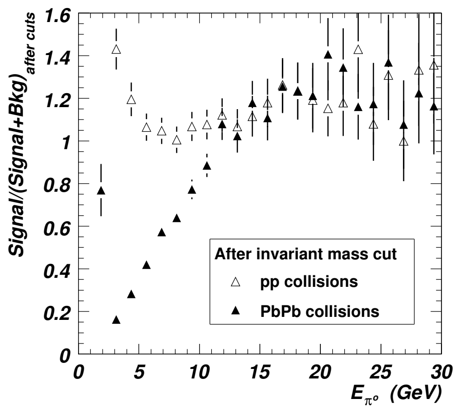

Fig. 7. Ratio of number of simulated π^0 to the total number of photon pairs satisfying the opening angle, invariant mass and leading particle selection conditions for pp ($\triangle$) and Pb-Pb ($\blacktriangle$) collisions at $\sqrt{s} = 5.5A$ TeV. Only γ-jet events in the jet energy range from 20 to 100 GeV are considered.

The condition $\theta \leq \theta_{max}$ selects more than 80% of the π^0 decay photon pairs[4] and rejects more than the 93% of all the uncorrelated photon pairs (Fig. 6). π^0 are finally identified by requiring the additional condition $120 < M_{\gamma\gamma} < 150$ MeV$/c^2$ on the invariant mass. The efficiency of the π^0 identification is calculated from the ratio of the number of simulated π^0 to the whole number of photon pairs produced in the heavy-ion event satisfying the selection conditions (Fig. 7). This ratio is between 1 and 1.2 for π^0 of energies greater than 5 GeV for pp collisions at $\sqrt{s} = 5.5$ TeV and 10 GeV for Pb-Pb collisions at $\sqrt{s} = 5.5A$ TeV. The ratio may be larger than one because the opening angle restriction eliminates a fraction of true π^0 decay pairs. The combinatorial background is responsible of the fast decrease of the signal to noise ratio in Pb-Pb collisions at low energies (Fig. 7).

[4] The selection efficiency decreases from about 92% at $E_\pi \sim 2$ GeV to around 82% at $E_\pi \sim 15$ GeV and then increases again to values larger than 90% for $E_\pi > 30$ GeV.

4 Jet reconstruction

Jets are reconstructed starting from the seed provided by the leading particle found as described above. Particles found in a cone around the leading particle at $(\eta_l,\ \phi_l)$, of size R defined by the equation,

$$R = \sqrt{(\phi_l - \phi)^2 + (\eta_l - \eta)^2}, \tag{3}$$

are assigned to a jet if their transverse momentum exceeds a given p_T^{th}. Again, a fraction of jet particles may be lost due to the limited detector acceptance. Only jets with reconstructed energy comparable to the energy of their corresponding prompt photon are selected.

In our jet finding algorithm, two experimental configurations are considered,

(1) Charged particles are detected in the central tracking system and neutral particles in EMCal. This configuration is labeled TPC+EMCal in figures and text.

(2) Only the central tracking system is available and consequently only charged particles can be detected; this configuration is labeled TPC in figures and text.

We compare in the upper part of Fig. 8 the ratio of the measured jet transverse momentum $p_{T,j}$ (p_T^{th}=0.5 GeV/c, $R = 0.3$) to the energy of the corresponding prompt photon E_γ for pp collisions and $E_\gamma = 40$ GeV and for both detector configurations. In the TPC+EMCal configuration, the jet energy is correctly reconstructed, and values close to the energy of the corresponding prompt photon are obtained. As the energy carried away by neutral particles can only be detected with EMCal, the $p_{T,j}/E_\gamma$ distribution does not show the expected correlation in the TPC configuration. The correlation is best observed for the highest jet energy studied. This result is independent of the cone size.

In the case of Pb-Pb collisions, the background is large and the $p_{T,j}/E_\gamma$ distributions are wide and peak at values greater than unity (middle part of Fig. 8). Requiring a higher p_T threshold than for pp collisions ($p_T^{th} = 2$ GeV/c) to reduce the background, the distribution features (peak position and width) resemble those obtained for pp collisions, at least for high-energy jets (lower part of Fig. 8). Although the width is still large for 20 GeV/c jets, imposing a higher p_T threshold produces a loss of essential information about the jet (2 GeV/c is already 10% of the jet energy). Consequently, the jet energy was calculated by requiring a p_T threshold of 0.5 GeV/c for pp collisions and of 2 GeV/c for Pb-Pb collisions. Nevertheless, to construct the jet fragmentation functions, as described in next sections, all detected particles with $p_T^{th} = 0.5$ GeV/c inside the cone were taken into account.

Photon-jet events are well identified with the setup including EMCal when the ratio $p_{T,j}/E_\gamma$ is close to one. Two different values were considered for the lower $p_{T,j}/E_\gamma$ limits, depending on the experimental setup (with or without EMCal). The optimal selection windows (Fig. 9), depend on the energy of the reconstructed jet.

The jet reconstruction algorithm fails for jets with $p_{T,j} < 10$ GeV/c due to the large fluctuations of the $p_{T,j}/E_\gamma$ ratio at low energies. Therefore, such jets were excluded from our investigations.

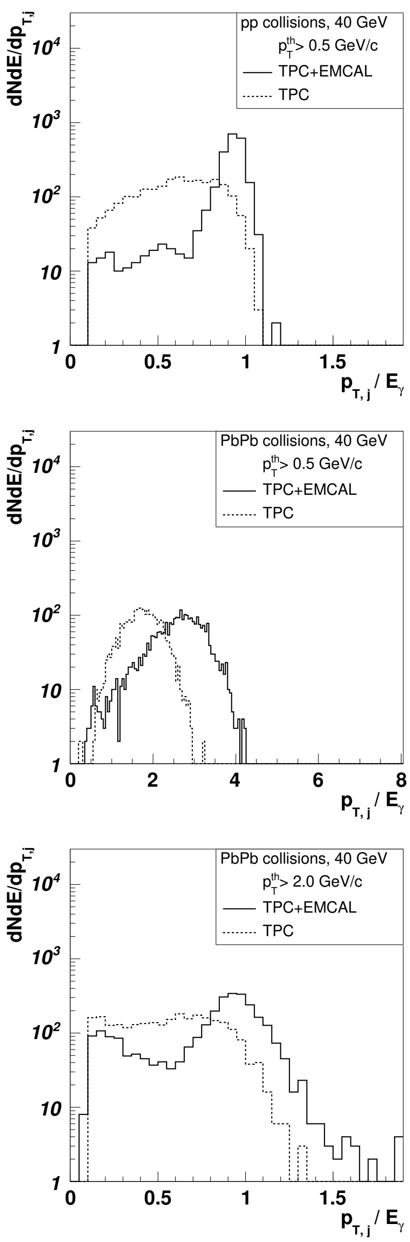

Fig. 8. Jet distribution as a function of the ratio $p_{T,j}/E_\gamma$ for generated γ-jet events in pp collisions (top frame) and Pb-Pb collisions (middle and bottom frames) at $\sqrt{s} = 5.5A$ TeV. A jet cone of $R = 0.3$ and a jet particle threshold of $p_T^{th} = 0.5$ GeV/c are required in the top and middle frames and a jet particle threshold of $p_T^{th} = 2$ GeV/c is taken in the lower one. Results for the setups without EMCal (dashed line) and with EMCal (solid line) are given.

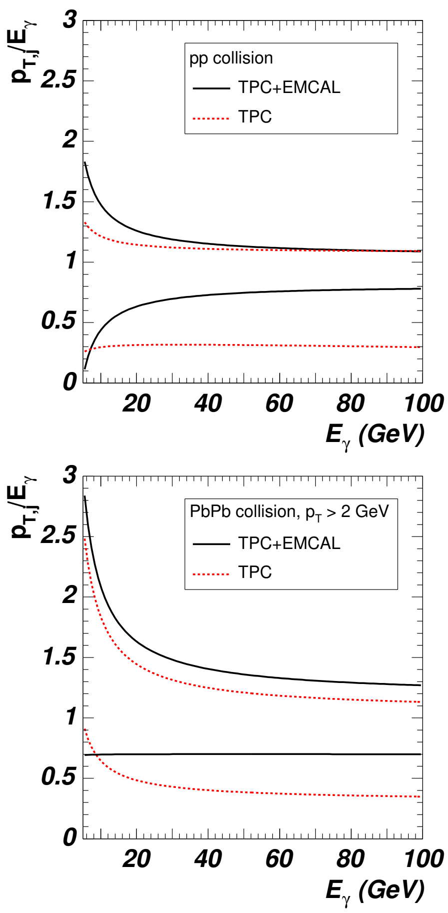

Fig. 9. Maximum (upper line) and minimum values (lower line) of the $p_{T,j}/E_\gamma$ ratio used to select photon-jet events in the configurations with EMCal (solid line) and without EMCal (dashed line) for pp at $\sqrt{s}$ = 5.5 TeV (upper figure) and Pb-Pb collisions at $\sqrt{s} = 5.5A$ TeV (lower figure).

5 Efficiency and contamination of jet selection

The jet selection efficiency is defined as the ratio of the number of identified γ-tagged jets to the number of prompt photons detected in PHOS (Fig. 10 for pp collisions and Fig. 11 for Pb-Pb collisions). The efficiency for the configuration with EMCal is about 30%. For the configuration without EMCal, the efficiency is higher (about 40-50%) due to the larger acceptance of the central tracking system. To estimate the contamination level of wrongly identified γ-jets from jet-jet events, we applied the γ-jet algorithm also to these events. This contamination originates mainly from the decay photons contained in jets reaching PHOS, which may be misidentified as prompt photons and provide a seed for the algorithm. Indeed, the contribution of these background prompt photons can be even larger than the contribution of true prompt photons [1]. When the γ-tagging algorithm is applied to jet-jet events, a substantial fraction of misidentified prompt photons is rejected. When no prompt photon identification is performed in PHOS, only about 10% of the jet-jet events are accepted in the setup with EMCal but the value raises to 40-50% in the absence of EMCal for both pp and Pb-Pb collisions (Figs. 10 and 11).

We studied the purity $\mathcal{P}$ and the contamination $\mathcal{C}$ of γ-jet identified events. The purity is defined as the fraction of true γ-jet events among the identified events and the contamination as the fraction of jet-jet events identified as γ-jet events, i.e., $\mathcal{C} = 1 - \mathcal{P}$. In a first step, the γ-tagging algorithm was triggered by every high-p_T neutral signal detected in PHOS. In the case of the TPC+EMCal configuration, purities of about 80% and 60% for pp and Pb-Pb collisions, respectively, were obtained (Fig. 12). Without EMCal, the purity was only of 20-40%. In a second step, the prompt photon identification was switched on by including a shower shape analysis (SSA) and an isolation cut method (ICM) [1]. A strong enhancement of the purity was obtained (Fig. 13). In the case of pp collisions, the purity was larger than 90% for the configuration without EMCal and about 99% for the configuration with EMCal. In the case of Pb-Pb collisions and for the configuration without EMCal the purity levels were about 80% in the whole energy range except between 30 and 50 GeV where the purity was about 90%. With EMCal the purity was higher than 90% in the entire energy range.

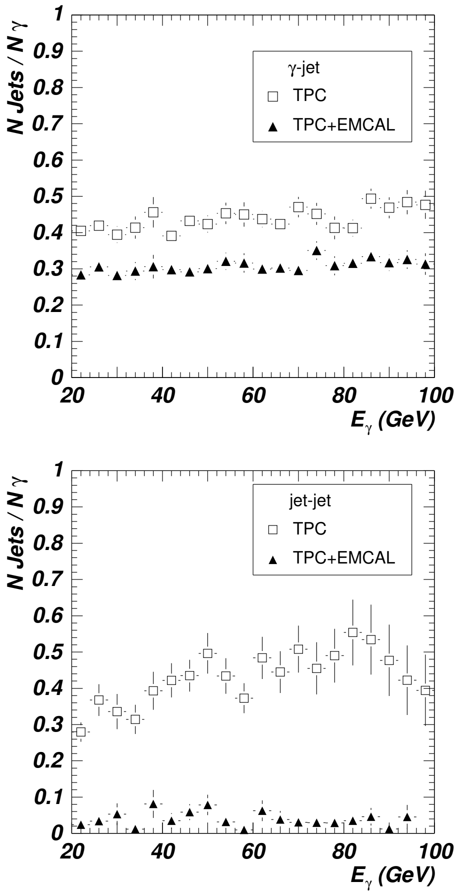

Fig. 10. Upper frame: Jet selection efficiency. Lower frame: Number of accepted jet-jet events divided by the number of γ-like particles detected in PHOS (not identified). Results for pp collisions and for the setups without EMCal (□) and with EMCal (▲).

6 Fragmentation functions

A well established method to study quantitatively the interaction of jets with the medium is to investigate the redistribution of fragmentation hadrons in phase space [4], i.e., to measure the jet fragmentation function. The experimental fragmentation function is the distribution of charged hadrons within jets as a function of the variable z, defined for hard processes with a γ-jet pair in the final state as $z = p_T/E_\gamma$. The statistics for the fragmentation function

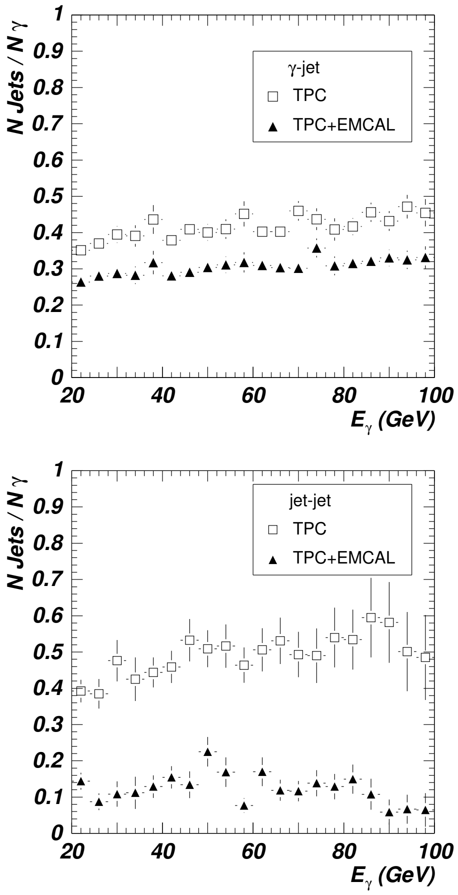

Fig. 11. Upper frame: Jet selection efficiency. Lower frame: Number of accepted jet-jet events divided by the number of γ-like particles detected in PHOS (not identified). Results for Pb-Pb collisions at $\sqrt{s} = 5.5A$ TeV and for the setups without EMCal ($\square$) and with EMCal ($\blacktriangle$).

measurement during a standard year of LHC running was estimated for both pp and Pb-Pb collisions at $\sqrt{s} = 5.5A$ TeV (Figs. 14 and 15). These fragmentation functions were constructed from γ-jet events and misidentified jet-jet events by integrating all events with identified prompt photon energy larger than 20 GeV/c. The following conclusions are obtained:

(1) In the case of pp collisions, in the absence of EMCal and without prompt photon identification, the contamination due to misidentified jet-jet events dominates the true γ-jet contribution. In the setup with EMCal the con-

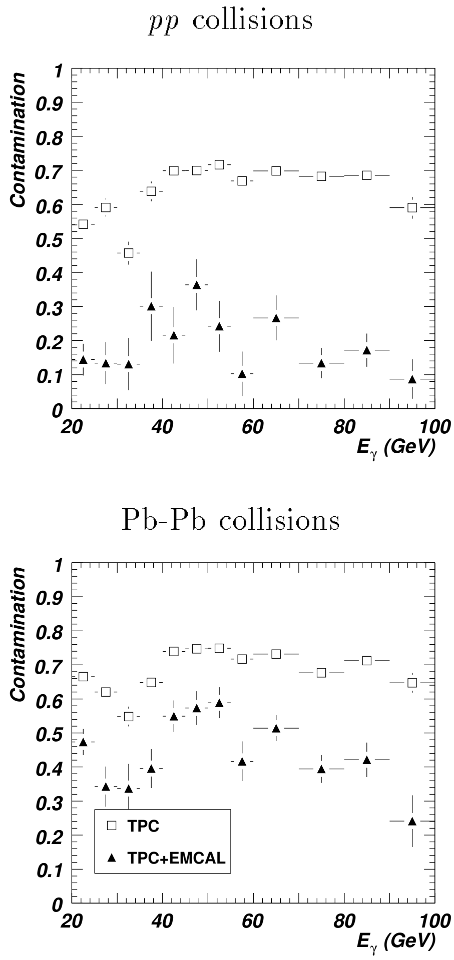

Fig. 12. γ-tagging contamination without prompt photon identification in PHOS, i.e., a high-p_T neutral signal triggers the jet finding algorithm. Upper (lower) frame corresponds to pp (Pb-Pb) collisions at $\sqrt{s} = 5.5A$ TeV. Results shown for the setups without EMCal (□) and with EMCal (▲).

tamination is suppressed, leading to a signal to background ratio close to 4. If prompt photons in PHOS are identified by medium purity SSA and ICMS (an isolation cut method with a threshold on the total p_T sum) [1], the contamination of misidentified jet-jet events is largely reduced, leading to a signal to background ratio of about 20 in the configuration without EMCal and near to 100% background rejection for the setup with EMCal. This reduction of background is accompanied by a reduction of

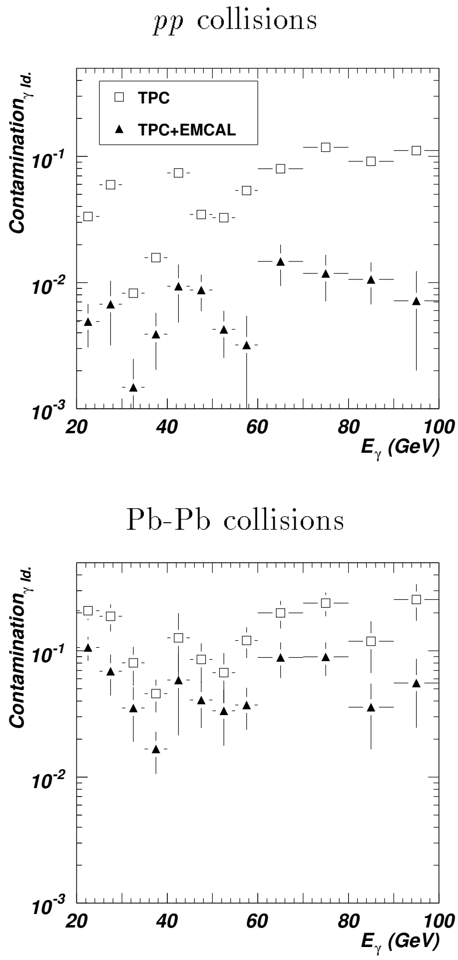

Fig. 13. γ-tagging contamination with prompt photon identification in PHOS (SSA+ICM, see definitions in Refs. [1,6]). Upper (lower) frame corresponds to pp (Pb-Pb) collisions at $\sqrt{s} = 5.5A$ TeV. Results shown for the setups without EMCal (□) and with EMCal (▲).

the γ-jet statistics of only 10%.

(2) In the case of Pb-Pb collisions, the measured fragmentation function presents a peak at low z, an artifact due to low-p_T charged hadrons coming from the heavy-ion underlying event. This peak can be statistically subtracted by calculating the contribution outside the cone defined by the leading particle. This contribution is estimated by constructing a pseudo-fragmentation function with the particles inside a cone (with the same R

pp collisions

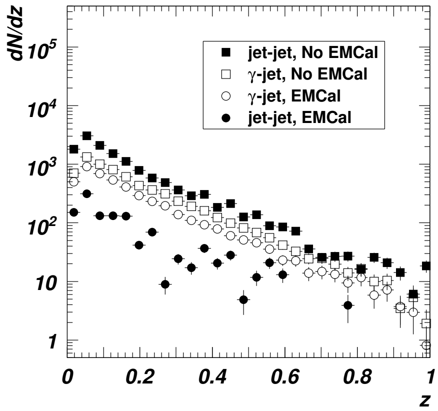

Pb-Pb collisions

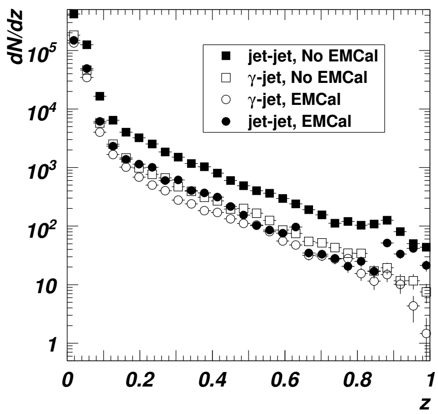

Fig. 14. Fragmentation function for γ-jet and jet-jet events with photon energy larger than 20 GeV for pp (upper frame) and Pb-Pb (lower frame) collisions at $\sqrt{s} = 5.5A$ TeV. Neither prompt photon identification in PHOS nor heavy-ion environment background subtraction are done.

as the jet cone) centered at $(\phi_\gamma, \eta_{leading})$ which for γ-jet events is a region populated only by particles coming from the HIJING event with no contribution from the jet. Prompt photon identification by medium purity SSA and ICM was required to reduce the contamination of wrongly identified jet-jet events to an acceptable level. The final signal to background ratio obtained is about 4 in the case without EMCal and rises up to 10 with EMCal. The requirement of prompt photon identification reduces

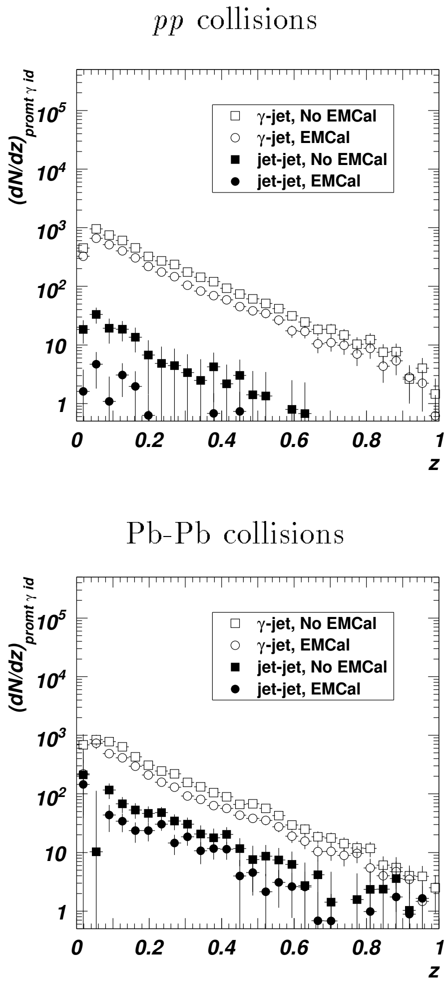

Fig. 15. Fragmentation function for γ-jet and jet-jet events with photon energy larger than 20 GeV for pp (upper frame) and Pb-Pb (lower frame) collisions at $\sqrt{s} = 5.5A$ TeV. Prompt photons are identified in PHOS by medium purity SSA and ICM (pp collisions) or ICMS (Pb-Pb collisions), and the heavy-ion background is statistically subtracted (see Refs. [1, 6] for details on identification definitions).

the statistics of γ-jet events by about 60%.

The fragmentation functions were calculated as the sum of the identified γ-jet events and jet-jet background events scaled by the corresponding cross section (Figs. 16 and 17). Statistical errors were calculated from the statistics that can be accumulated in a standard LHC year of running. Systematic errors reflect the amount of contamination. For Pb-Pb collision, in the range $0.1 < z < 0.5$,

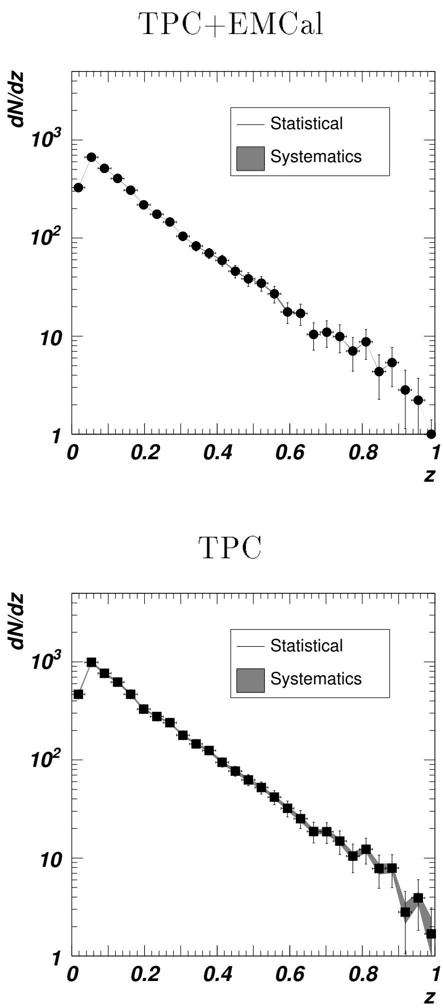

Fig. 16. Fragmentation function for γ-tagged jets (γ-jet + jet-jet events after prompt photon identification) with photon energy larger than 20 GeV for a whole ALICE year, detected in the central tracking system and EMCal (upper frame) and in the central tracking system alone (lower frame), for pp collisions. The shaded regions represent the systematic error due to jet-jet contamination.

systematic and statistical errors are of the same order, both with and without EMCal. Statistical errors outside this z range are too large to measure medium modifications effects. The inclusion of EMCal reduces the systematic errors by a factor of about 5 in pp collisions and about 2 in Pb-Pb collisions. When high p_T π^0 suppression as observed at RHIC [12–15] is accounted for, systematic errors are additionally reduced by a factor 5, becoming thus systematically

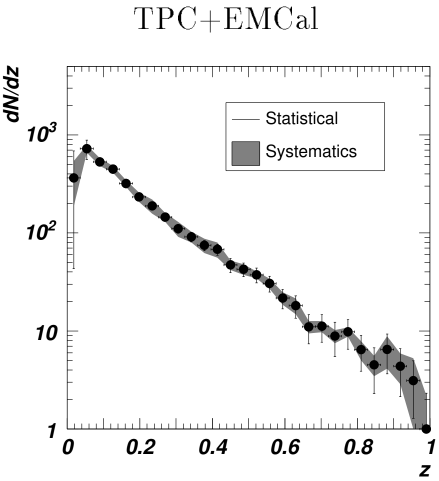

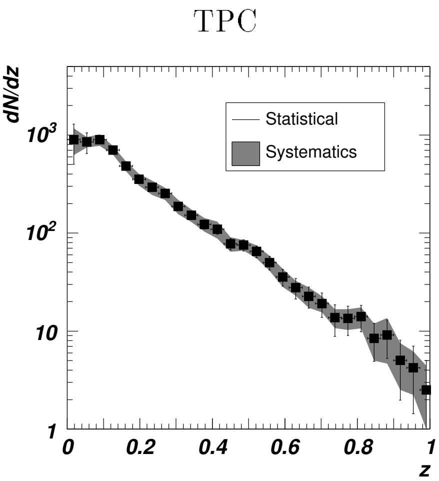

Fig. 17. Fragmentation function for γ-tagged jets (γ-jet + jet-jet events after prompt photon identification) with photon energy larger than 20 GeV for a whole ALICE year, detected in the central tracking system and EMCal (upper frame) and in the central tracking system alone (lower frame), for Pb-Pb collisions at $\sqrt{s} = 5.5A$ TeV. The shaded regions represent the systematic error due to jet-jet contamination.

smaller than the statistical errors, both with and without EMCal.

The sensitivity of photon-tagged jet fragmentation functions to nuclear medium modifications can be estimated from the nuclear modification factor R_{FF}. This factor is defined as the ratio of the fragmentation functions measured in AA and pp collisions scaled to the number of binary NN collisions, with both

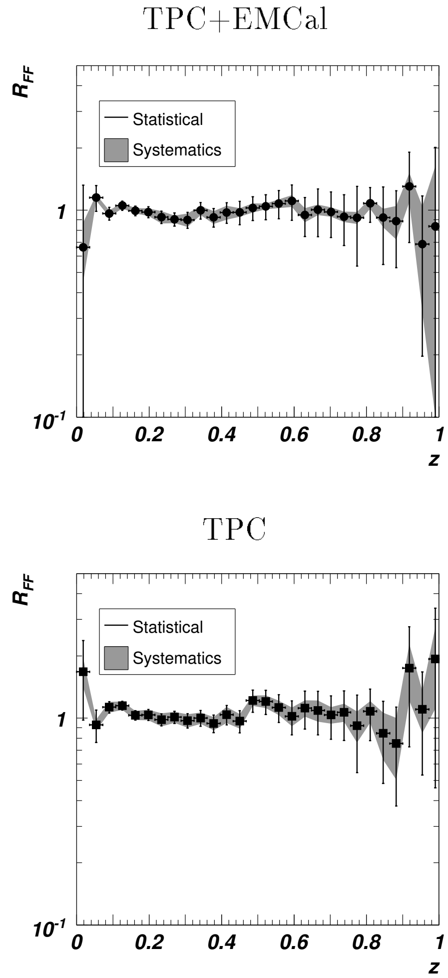

Fig. 18. Ratio of the fragmentation functions of γ-tagged jets with photon energy larger than 20 GeV for Pb-Pb collisions at $\sqrt{s} = 5.5A$ TeV scaled by the number of binary collisions [1] to pp collisions at $\sqrt{s} = 5.5$ TeV detected in the central tracking system and EMCal (upper frame) or in the central tracking system alone (lower frame). The shaded region represents the systematic error due to contamination from jet-jet events.

fragmentation functions calculated for the same beam luminosity and running time. R_{FF} should be equal to unity in the absence of nuclear effects. As no medium modification effect was included in our simulations, we obtain indeed a value close to one over the entire z range (Fig. 18). The statistical and systematic errors indicate that variations of R_{FF} larger than 5% could be

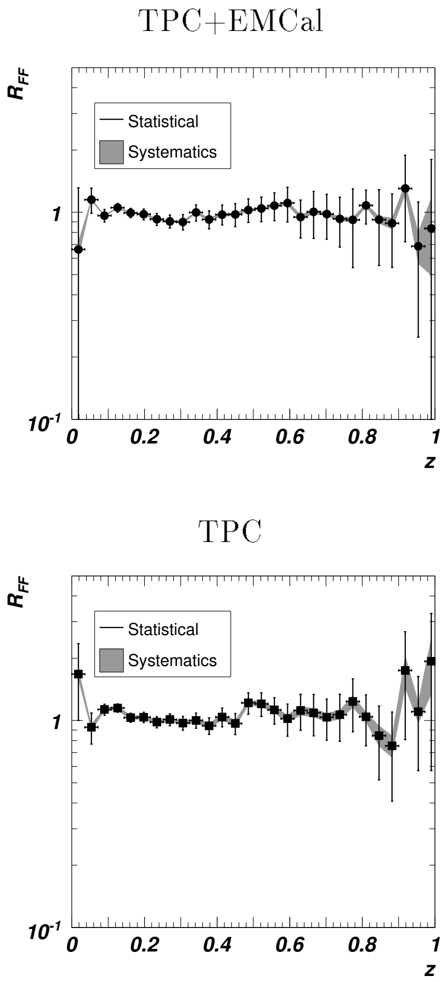

Fig. 19. Ratio of the fragmentation functions of γ-tagged jets with photon energy larger than 20 GeV for Pb-Pb collisions at $\sqrt{s} = 5.5A$ TeV scaled by the number of binary collisions [1] to pp collisions at $\sqrt{s} = 5.5$ TeV detected in the central tracking system and EMCal (upper frame) or in the central tracking system alone (lower frame). The shaded region represents the systematic error due to the contamination from jet-jet events. Background is quenched a factor 5 like at RHIC.

measured for both setups in the range $0.1 < z < 0.5$. If π^0 are quenched by a factor of 5, as observed at RHIC, the systematic error would be smaller than 5% for both setups, as displayed in Fig. 19. However, there is no possibility to measure the nuclear modification factor with an accuracy better than 5% due to limited γ-jet statistics expected in one year of data taking.

We may still consider another measurement approach in which prompt photons are detected by EMCal and jets are only measured by the central tracking system [5]. In this setup, the prompt photon counting rate would be enhanced by a factor of 7 and consequently the statistical errors would be reduced by a factor 2.6 (figures obtained by assuming the responses of PHOS and EMCal identical). This reduction of statistical errors may allow to measure medium modification effects over a wider z range.

7 Conclusions

We have developed an algorithm to identify γ-jet events generated in pp and Pb-Pb collisions at $\sqrt{s} = 5.5A$ TeV with the LHC detector ALICE. The γ-jet events are identified by selecting a prompt photon in PHOS and searching for the leading particle in the opposite direction inside the ALICE central tracking system. Two different setups, with and without the electromagnetic calorimeter EMCal, are considered. Jets are reconstructed by an algorithm in which the leading particle is used as a seed. The reconstructed jet is correlated to the photon if a number of conditions are fulfilled. The efficiency of identifying γ-jet events is mainly determined by the acceptance of the central tracking system and EMCal. For jets of energy larger than 20 GeV, this efficiency is found to be from around 40% to 50% with increasing photon energy without EMCal, and, due to the smaller EMCal acceptance, about 30% with EMCal. A large contribution to the γ-jet event background comes from π^o decay photons misidentified in PHOS as prompt photons. With our γ-jet

[5] It is not advisable to use PHOS as a detector of jet neutral particles due to its reduced acceptance.

tagging method in combination with isolation cut analysis for prompt photon identification, the misidentification of jet-jet events as γ-jet events in pp collisions is of the order of 5% without EMCal and less than 1% with EMCal, and in Pb-Pb collisions is of the order of 20% without EMCal and around 10% with EMCal. We obtain from our simulations that fragmentation functions could be measured with sufficient accuracy to obtain the nuclear modification factor R_{FF} with errors low enough to probe medium modifications. As a main conclusion, we find that nuclear medium modifications could be measured if they produce variations of R_{FF} larger than 5% in the region $0.1 < z < 0.5$.

8 Acknowledgment

This work has been supported in part by the Spanish DGICYT under contract FPA2003-07581-C02-01. One of us (G. C.) thanks Ministerio de Educación y Ciencia for a PhD fellowship contract FP200-5452 and the Marie Curie EU program for the "Training Site" contract HPMT-CT-2001-00346. Also, we thank the support of the INTAS grant 03-52-5747.

References

[1] G. Conesa et al., Nucl. Instr. and Meth. A580 (2007) 1446.

[2] A. Accardi et al, hep-ph/0310274 (2004).

[3] J.D. Bjorken, FERMILAB-PUB-82-059-THY (1982).

[4] C. A. Salgado and U.A. Wiedemann, Phys. Rev. Lett. **93** (2004) 42301.

[5] F. Arleo et al., JHEP **11** (2004) 009.

[6] ALICE Collaboration et al., *Physics performace report, Volume II*, J. Phys. G: Nucl. Part. Phys. **32** (2006) 1295-2040

[7] T. Sjostrand et al., *Comput. Phys. Commun.* **135** (2001) 238-259.

[8] T. Sjostrand et al., *PYTHIA 6.2: Physics and manual*, hep-ph/0108264 (2001).

[9] M. Gyulassy and X.N. Wang, *Comput. Phys. Commun.* **83** (1994) 307–331.

[10] ALICE Collaboration, *J. Phys. G: Nucl. Part. Phys.* **30** (2004)1517-1763.

[11] T. Cormier et al., Eur Phys J, **C 34**, (2004) s01, s333-345

[12] J. Adams et al., the STAR collaboration, Nucl. Phys. **A757** (2005) 102.

[13] K. Adcox et al., thePHENIX collaboration, Nucl. Phys. **A757** (2005) 184.

[14] I. Arsene et al., the BRAHMS collaboration, Nucl. Phys. **A757** (2005) 1.

[15] M. B. Tonjes et al., PHOBOS collaboration, Nucl. Phys. **A757** (2005) 61.